INTERNATIONAL JOURNAL FOR NUMERICAL METHODS IN FLUIDS
Int. J. Numer. Meth. Fluids 2007; **55**:1019–1038
Published online 1 May 2007 in Wiley InterScience (www.interscience.wiley.com). DOI: 10.1002/fld.1504

An explicit formulation for the evolution of nonlinear surface waves interacting with a submerged body

Christopher P. Kent[1,*,†] and Wooyoung Choi[2]

[1]*Department of Marine and Environmental Systems, Florida Institute of Technology, Melbourne, FL 32901, U.S.A.*
[2]*Department of Mathematical Sciences, Center for Applied Mathematics and Statistics, New Jersey Institute of Technology, Newark, NJ 07102, U.S.A.*

SUMMARY

An explicit formulation to study nonlinear waves interacting with a submerged body in an ideal fluid of infinite depth is presented. The formulation allows one to decompose the nonlinear wave–body interaction problem into body and free-surface problems. After the decomposition, the body problem satisfies a modified body boundary condition in an unbounded fluid domain, while the free-surface problem satisfies modified nonlinear free-surface boundary conditions. It is then shown that the nonlinear free-surface problem can be further reduced to a closed system of two nonlinear evolution equations expanded in infinite series for the free-surface elevation and the velocity potential at the free surface. For numerical experiments, the body problem is solved using a distribution of singularities along the body surface and the system of evolution equations, truncated at third order in wave steepness, is then solved using a pseudo-spectral method based on the fast Fourier transform. A circular cylinder translating steadily near the free surface is considered and it is found that our numerical solutions show excellent agreement with the fully nonlinear solution using a boundary integral method. We further validate our solutions for a submerged circular cylinder oscillating vertically or fixed under incoming nonlinear waves with other analytical and numerical results. Copyright © 2007 John Wiley & Sons, Ltd.

Received 2 June 2006; Revised 12 March 2007; Accepted 13 March 2007

KEY WORDS: pseudo-spectral; waves; free surface

1. INTRODUCTION

Nonlinear inviscid calculations for wave–body interaction problems have been predominantly based on the mixed Eulerian–Lagrangian (MEL) boundary integral approach, originally proposed by Longuet-Higgins and Cokelet [1]. See, for example, the review by Beck and Reed [2] for the

*Correspondence to: Christopher P. Kent, Department of Marine and Environmental Systems, Florida Institute of Technology, Melbourne, FL 32901, U.S.A.
†E-mail: ckent@fit.edu

Contract/grant sponsor: US Office of Naval Research; contract/grant number: N00014-05-1-0537

Copyright © 2007 John Wiley & Sons, Ltd.

application of a MEL method to wave–body interaction problems, and see Liu *et al.* [3] for a recent three-dimensional result. Despite significant improvements over recent decades, the MEL-type method is still computationally expensive for practical applications and it is desirable to have a new efficient and accurate numerical scheme.

As an alternative numerical approach to solve wave–body interaction problems, Liu *et al.* [4] generalized the higher-order spectral (HOS) method, originally introduced for free wave problems by Dommermuth and Yue [5]. In this approach, the free-surface boundary conditions are expanded about the mean free surface and the resulting linear boundary value problems of wave–body interaction at each order of wave steepness are solved numerically using a pseudo-spectral method based on the fast Fourier transform (FFT). The free-surface variables such as the free-surface elevation and the free-surface velocity potential are then updated by solving the nonlinear evolution equations using a pseudo-spectral method. The HOS method has been also adopted by Liu *et al.* [6] and Lin and Kuang [7].

Although the HOS approach has been found to be numerically efficient compared with the MEL approach, it is still cumbersome because, at every time step, before the free-surface variables are evolved, one must numerically solve a separate boundary value problem for each order of nonlinearity. Here, to solve nonlinear wave–body interaction problems more efficiently, we present an improved formulation which requires one to solve a linear boundary value problem in an unbounded fluid domain (with no free surface present) only once per time step for any order of approximation, and provides nonlinear evolution equations, explicitly written to the desired order, for the free-surface variables defined in the horizontal plane.

Combined with an asymptotic expansion similar to that used by Choi [8] for free wave problems, it is shown that the wave–body interaction problem can be decomposed into the body problem satisfying the modified body boundary condition on the instantaneous body surface in an unbounded domain and the free-surface problem that is reduced to solving a closed set of nonlinear evolution equations for the free-surface variables written in infinite series. The body problem is then solved numerically using a distribution of singularities, while the explicit evolution equations are solved using a pseudo-spectral method based on the FFT. In the absence of a body, when written in Fourier space, the evolution equations are reduced to those of West *et al.* [9] and, therefore, the formulation presented here can be regarded as a generalization of that of West *et al.* [9] for wave–body interaction problems.

After describing our formulation in Sections 2–4 and numerical method in Section 5, we present the steady translation as well as the radiation and diffraction problems for a submerged circular cylinder. Whenever possible, we compare our results with experimental, theoretical or other numerical results.

2. GOVERNING EQUATIONS

For an ideal fluid of density ρ, the velocity potential $\phi(\mathbf{x}, z, t)$ for a free-surface flow with a body present can be found by solving the following nonlinear boundary value problem:

$$\nabla^2\phi + \frac{\partial^2\phi}{\partial z^2} = 0 \quad \text{for } -\infty \leqslant z \leqslant \zeta(\mathbf{x}, t) \tag{1}$$

$$\frac{\partial\zeta}{\partial t} + \nabla\phi \bullet \nabla\zeta = \frac{\partial\phi}{\partial z} \quad \text{at } z = \zeta(\mathbf{x}, t) \tag{2}$$

Copyright © 2007 John Wiley & Sons, Ltd.

DOI: 10.1002/fld

$$\frac{\partial\phi}{\partial t}+\frac{1}{2}|\nabla\phi|^2+\frac{1}{2}\left(\frac{\partial\phi}{\partial z}\right)^2+g\zeta=0 \quad \text{at } z=\zeta(\mathbf{x},t) \tag{3}$$

$$|\nabla_3\phi|\to 0 \quad \text{as } z\to-\infty \tag{4}$$

$$\frac{\partial\phi}{\partial n}=\mathbf{V}\cdot\mathbf{n} \quad \text{on } S_B(t) \tag{5}$$

where g is the gravitational acceleration, $\zeta(\mathbf{x},t)$ is the free-surface elevation, $\mathbf{x}=(x,y)$, and ∇ and ∇_3 are the two- and three-dimensional gradients, respectively, defined by

$$\nabla=\left(\frac{\partial}{\partial x},\frac{\partial}{\partial y}\right), \quad \nabla_3=\left(\nabla,\frac{\partial}{\partial z}\right) \tag{6}$$

In the body boundary condition (5), $\mathbf{V}$ is the velocity of the body surface, $\mathbf{n}$ is the normal vector directed into the body, and $S_B(t)$ represents the instantaneous body position. At lateral boundaries, either zero flux at infinity or periodic boundary conditions can be imposed. Here, we have assumed that surface tension can be neglected, and that no external pressure is applied to the fluid.

By substituting $z=\zeta$ into (2) and (3), and using the following chain rule for differentiation, the kinematic and dynamic free-surface boundary conditions can be written in terms of the surface elevation ζ and the free-surface velocity potential $\Phi\equiv\phi(\mathbf{x},\zeta,t)$ as

$$\frac{\partial\zeta}{\partial t}+\nabla\Phi\cdot\nabla\zeta=(1+|\nabla\zeta|^2)W \tag{7}$$

$$\frac{\partial\Phi}{\partial t}+\frac{1}{2}(\nabla\Phi)^2+g\zeta=\frac{1}{2}(1+|\nabla\zeta|^2)W^2 \tag{8}$$

If one can find the expression, in terms of the free-surface variables, ζ and Φ, for the vertical velocity evaluated at the free surface, W, defined as

$$W=\left.\frac{\partial\phi}{\partial z}\right|_{z=\zeta} \tag{9}$$

Equations (7)–(8) can be considered a closed system of two coupled evolution equations for these two free-surface variables. In order to close the system, following West *et al.* [9], Φ and W are expanded in Taylor series about $z=0$

$$\Phi(\mathbf{x},t)=\sum_{n=0}^{\infty}(-1)^n\frac{\zeta^{2n}}{(2n)!}\triangle^n\phi_0+\sum_{n=0}^{\infty}(-1)^n\frac{\zeta^{2n+1}}{(2n+1)!}\triangle^n w_0 \tag{10}$$

$$W(\mathbf{x},t)=\sum_{n=0}^{\infty}(-1)^n\frac{\zeta^{2n}}{(2n)!}\triangle^n w_0+\sum_{n=0}^{\infty}(-1)^{n+1}\frac{\zeta^{2n+1}}{(2n+1)!}\triangle^{n+1}\phi_0 \tag{11}$$

where we have used $\partial^2\phi/\partial z^2=-\nabla^2\phi$, $\triangle=\nabla^2$, and

$$\phi_0=\phi(\mathbf{x},0,t), \quad w_0=\frac{\partial\phi}{\partial z}(\mathbf{x},0,t) \tag{12}$$

Once the relationship between ϕ_0 and w_0 is found, as described in Section 3, one can first invert the series for Φ given by (10) and then substitute the inverted series for ϕ_0 into (11) to obtain the expression for W in terms of Φ and ζ.

Copyright © 2007 John Wiley & Sons, Ltd.

DOI: 10.1002/fld

3. DECOMPOSITION OF THE TOTAL VELOCITY POTENTIAL

In order to find the relationship between ϕ_0 and w_0, both defined at the mean free surface ($z=0$), we consider the following linear boundary value problem:

$$\left(\nabla^2 + \frac{\partial^2}{\partial z^2}\right)\phi = 0 \quad \text{for } -\infty < z < 0 \tag{13}$$

$$\phi = \phi_0(\mathbf{x}, t) \quad \text{at } z = 0 \tag{14}$$

$$|\nabla_3 \phi| \to 0 \quad \text{as } z \to -\infty \tag{15}$$

$$\frac{\partial \phi}{\partial n} = \mathbf{V} \cdot \mathbf{n} \quad \text{on } S_{\mathrm{B}}(t) \tag{16}$$

Note that a simple linear boundary condition (or the definition of ϕ_0) is imposed at the mean free surface in this auxiliary problem since the original free-surface boundary conditions given by (7)–(8) will be satisfied automatically when the nonlinear evolution equations, with substituting the expression for W in terms of ζ and Φ into (7)–(8), are solved.

To solve (13)–(16), one can further decompose the velocity potential ϕ into

$$\phi = \phi^{\mathrm{F}} + \phi^{\mathrm{B}} \tag{17}$$

where ϕ^{F} and ϕ^{B} are the solutions of the free-surface and body problems, respectively. For the free-surface problem, we choose to impose a boundary condition at the mean free surface, but no boundary condition on the body surface for ϕ^{F}; and *vice versa* in the body problem for ϕ^{B}, as illustrated in Figure 1. When these two problems are superimposed, the auxiliary problem should be recovered. Although this choice of the decomposition into the free-surface and body problem potentials is not unique, an advantage of this decomposition is that the body problem is greatly

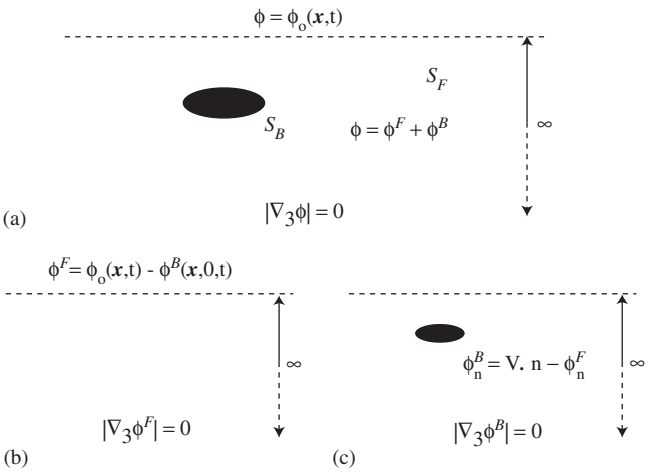

Figure 1. Decomposition of the original problem into the free-surface and body problems: (a) original problem; (b) free-surface problem; and (c) body problem.

Copyright © 2007 John Wiley & Sons, Ltd.

DOI: 10.1002/fld

simplified to one in an unbounded domain which can be easily solved. Another alternative, for example, is to impose a simple free-surface boundary condition for the body problem, e.g. $\phi^{\mathrm{B}}=0$ at $z=0$, so that the free-surface boundary condition becomes simpler ($\phi^{\mathrm{F}}=\phi_0$ at $z=0$) in the free-surface problem, as used in Choi and Kent [10].

3.1. Free-surface velocity potential

With the decomposition shown in Figure 1, the free-surface velocity potential ϕ^{F} is the solution of the following boundary value problem:

$$\left(\nabla^2+\frac{\partial^2}{\partial z^2}\right)\phi^{\mathrm{F}}=0 \quad \text{for } -\infty<z<0 \tag{18}$$

$$\phi^{\mathrm{F}}=\phi_0(\mathbf{x},t)-\phi^{\mathrm{B}}(\mathbf{x},0,t) \quad \text{at } z=0 \tag{19}$$

$$|\nabla_3\phi^{\mathrm{F}}|\to 0 \quad \text{as } z\to-\infty \tag{20}$$

where ϕ_0 is the velocity potential at the mean free surface defined by (12), and the body velocity potential ϕ^{B} is the solution of the body problem. By using the Fourier transform defined by

$$\overline{\phi^{\mathrm{F}}}(\mathbf{k},z,t)\equiv\int_{-\infty}^{\infty}\phi^{\mathrm{F}}(\mathbf{x},z,t)\,\mathrm{e}^{\mathrm{i}\mathbf{k}\cdot\mathbf{x}}\,\mathrm{d}\mathbf{x} \tag{21}$$

where $\mathbf{k}=(k_1,k_2)$, the solution of (18)–(20) in the transformed plane can be found as

$$\overline{\phi^{\mathrm{F}}}=(\overline{\phi_0}(\mathbf{k},t)-\overline{\phi^{\mathrm{B}}}(\mathbf{k},0,t))\,\mathrm{e}^{kz} \tag{22}$$

where $k=({k_1}^2+{k_2}^2)^{1/2}$. Then, the Fourier transform of the total vertical velocity at the mean position $w_0(\mathbf{x},t)$ can be written as

$$\overline{w_0}(\mathbf{k},t)=\left.\overline{\frac{\partial\phi^{\mathrm{F}}}{\partial z}}\right|_{z=0}+\left.\overline{\frac{\partial\phi^{\mathrm{B}}}{\partial z}}\right|_{z=0}=k\overline{\phi_0}+\overline{f^{\mathrm{B}}} \tag{23}$$

and its inverse transform yields the relationship between w_0 and ϕ_0 as

$$w_0(\mathbf{x},t)=-\mathscr{L}[\phi_0]+f^{\mathrm{B}}(\mathbf{x},t) \tag{24}$$

In (24), the linear integral operator $\mathscr{L}$ [8] is defined as

$$\mathscr{L}[\Phi]=\frac{1}{2\pi}\int\!\!\int_{-\infty}^{\infty}\frac{(\mathbf{x}'-\mathbf{x})\bullet\nabla\Phi}{|\mathbf{x}'-\mathbf{x}|^3}\,\mathrm{d}x'\,\mathrm{d}y' \tag{25}$$

or, when acting on a Fourier component, as

$$\mathscr{L}[\mathrm{e}^{\mathrm{i}\mathbf{k}\cdot\mathbf{x}}]=-|\mathbf{k}|\,\mathrm{e}^{\mathrm{i}\mathbf{k}\cdot\mathbf{x}} \tag{26}$$

and f^{B} represents the effects of the body potential at the mean free surface as

$$f^{\mathrm{B}}(\mathbf{x},t)=\left.\frac{\partial\phi^{\mathrm{B}}}{\partial z}\right|_{z=0}+\mathscr{L}[\phi^{\mathrm{B}}]|_{z=0} \tag{27}$$

which can be computed after solving the body problem, as described below.

Copyright © 2007 John Wiley & Sons, Ltd.

DOI: 10.1002/fld

3.2. Body velocity potential

By subtracting (18)–(20) from (13)–(16), the body problem for ϕ^{B} is defined by

$$\left(\nabla^2 + \frac{\partial^2}{\partial z^2}\right)\phi^{\mathrm{B}} = 0 \quad \text{for } -\infty \leqslant z \leqslant 0 \tag{28}$$

$$|\nabla_3 \phi^{\mathrm{B}}| \to 0 \quad \text{as } z \to -\infty \tag{29}$$

$$\frac{\partial \phi^{\mathrm{B}}}{\partial n} = \mathbf{V} \cdot \mathbf{n} - \frac{\partial \phi^{\mathrm{F}}}{\partial n} \quad \text{on } S_{\mathrm{B}}(t) \tag{30}$$

where $\phi^{\mathrm{F}}(\mathbf{x}, z, t)$ is given by (22) for known $\phi_0(\mathbf{x}, t)$ (see also Equation (56)). Compared with the original governing equations given by (1)–(5), there are a couple of unique features in this form of the body problem. First, the body velocity potential can be obtained by solving a linear problem in an unbounded domain. Secondly, since the domain of interest is unbounded, there is no need to introduce free-surface Green functions, whose evaluation is computationally expensive. The solution of (28)–(30) can be found by various methods including a distribution of singularities, Green's identity, the multipole expansion method, etc. For example, ϕ^{B} can be represented by a distribution of singularities as

$$\phi^{\mathrm{B}}(\mathbf{x}, z, t) = \int_{S_{\mathrm{B}}} \sigma(\mathbf{x}', t) G(\mathbf{x}, \mathbf{x}', z, z')\, \mathrm{d}S' \tag{31}$$

where σ is determined by imposing the body boundary condition (30) at the instantaneous body position, and the Green function $G(\mathbf{x}', \mathbf{x})$ for three-dimensional flows is given by

$$G = -\frac{1}{4\pi} \frac{1}{[|\mathbf{x} - \mathbf{x}'|^2 + (z - z')^2]^{1/2}} \tag{32}$$

representing the velocity potential for a source located at $(\mathbf{x}', z')$. For two-dimensional flows, the Green function for a source at (x', z') is given by

$$G = \frac{1}{4\pi} \ln[(x - x')^2 + (z - z')^2] \tag{33}$$

4. EVOLUTION EQUATIONS FOR THE FREE-SURFACE VARIABLES

After solving the body problem for ϕ^{B} and evaluating $f^{\mathrm{B}}(\mathbf{x}, t)$, defined by (27), the relationship between ϕ_0 and w_0 can be obtained from (24) and, then, W can be expressed in terms of ζ and Φ from (10)–(11) by following the method described by Choi *et al.* [11] for free waves in the absence of a body.

After writing the Taylor series expansion for Φ given by (10) in the form of

$$\Phi = \sum_{n=0}^{\infty} \mathscr{A}_n[\phi_0] + \sum_{n=0}^{\infty} \alpha_n[f^{\mathrm{B}}] \tag{34}$$

Copyright © 2007 John Wiley & Sons, Ltd.

DOI: 10.1002/fld

where operators $\mathscr{A}_n$ and α_n are defined by, for even $n=2m$,

$$\mathscr{A}_{2m}=(-1)^m\frac{\zeta^{2m}}{(2m)!}\triangle^m,\quad \alpha_{2m}=0\quad \text{for } m=0,1,2,\ldots \tag{35}$$

for odd $n=2m+1$,

$$\begin{aligned}\mathscr{A}_{2m+1}&=(-1)^{m+1}\frac{\zeta^{2m+1}}{(2m+1)!}\triangle^m\mathscr{L}\\ \alpha_{2m+1}&=(-1)^m\frac{\zeta^{2m+1}}{(2m+1)!}\triangle^m\quad \text{for } m=0,1,2,\ldots\end{aligned} \tag{36}$$

one can find, by direct inversion, that

$$\phi_0=\sum_{n=0}^{\infty}\mathscr{B}_n[\Phi]+\sum_{n=0}^{\infty}\beta_n[f^{\mathrm{B}}] \tag{37}$$

where operators $\mathscr{B}_n$ and β_n can be found by the following recursion formulae:

$$\mathscr{B}_0=1,\quad \mathscr{B}_n=-\sum_{j=0}^{n-1}\mathscr{A}_{n-j}\mathscr{B}_j\quad \text{for } n\geqslant 1,\quad \beta_n=-\sum_{j=0}^{n}\mathscr{B}_{n-j}\alpha_j \tag{38}$$

Then, by substituting (37) into the series expansion for W given by

$$W=\sum_{n=0}^{\infty}\mathscr{C}_n[\phi_0]+\sum_{n=0}^{\infty}\gamma_n[f^{\mathrm{B}}] \tag{39}$$

where operators $\mathscr{C}_n$ and γ_n are defined by

$$\mathscr{C}_{2m}=(-1)^{m+1}\frac{\zeta^{2m}}{(2m)!}\triangle^m\mathscr{L},\quad \gamma_{2m}=A_{2m}\quad \text{for } n=2m\ (m=0,1,2,\ldots) \tag{40}$$

$$\mathscr{C}_{2m+1}=(-1)^{m+1}\frac{\zeta^{2m+1}}{(2m+1)!}\triangle^{m+1},\quad \gamma_{2m+1}=0\quad \text{for } n=2m+1\ (m=0,1,2,\ldots) \tag{41}$$

W can be expressed in terms of Φ and ζ as

$$W=\sum_{n=0}^{\infty}\mathscr{D}_n[\Phi]+\sum_{n=0}^{\infty}\delta_n[f^{\mathrm{B}}] \tag{42}$$

where operators $\mathscr{D}_n$ and δ_n are defined by

$$\mathscr{D}_n=\sum_{j=0}^{n}\mathscr{C}_{n-j}\mathscr{B}_j,\quad \delta_n=\gamma_n+\sum_{j=0}^{n}\mathscr{C}_{n-j}\beta_j \tag{43}$$

Copyright © 2007 John Wiley & Sons, Ltd.

DOI: 10.1002/fld

Finally, by substituting (42) into the free-surface boundary conditions given by (7)–(8), one can find the exact evolution equations for ζ and Φ

$$\frac{\partial \zeta}{\partial t} = Q(\zeta, \Phi) \equiv \sum_{n=1}^{\infty} Q_n(\zeta, \Phi) \tag{44}$$

$$\frac{\partial \Phi}{\partial t} = R(\zeta, \Phi) \equiv \sum_{n=1}^{\infty} R_n(\zeta, \Phi) \tag{45}$$

where Q_n and R_n are given by

$$\begin{aligned}
&Q_1 = \mathscr{D}_0[\Phi] + \delta_0[f^{\mathrm{B}}] \\
&Q_2 = -\nabla\Phi \bullet \nabla\zeta + \mathscr{D}_1[\Phi] + \delta_1[f^{\mathrm{B}}] \\
&Q_n = \mathscr{D}_{n-1}[\Phi] + \delta_{n-1}[f^{\mathrm{B}}] + |\nabla\zeta|^2(\mathscr{D}_{n-3}[\Phi] + \delta_{n-3}[f^{\mathrm{B}}]) \quad \text{for } n \geqslant 3
\end{aligned} \tag{46}$$

$$\begin{aligned}
&R_1 = -g\zeta \quad R_2 = -\tfrac{1}{2}|\nabla\Phi|^2 + \tfrac{1}{2}(\mathscr{D}_0[\Phi] + \delta_0[f^{\mathrm{B}}])^2 \\
&R_3 = (\mathscr{D}_0[\Phi] + \delta_0[f^{\mathrm{B}}])(\mathscr{D}_1[\Phi] + \delta_1[f^{\mathrm{B}}]) \\
&R_n = \frac{1}{2}\sum_{j=0}^{n-2}(\mathscr{D}_{n-j-2}[\Phi] + \delta_{n-j-2}[f^{\mathrm{B}}])(\mathscr{D}_j[\Phi] + \delta_j[f^{\mathrm{B}}]) \\
&\qquad + \frac{1}{2}|\nabla\zeta|^2 \sum_{j=0}^{n-4}(\mathscr{D}_{n-j-4}[\Phi] + \delta_{n-j-4}[f^{\mathrm{B}}])(\mathscr{D}_j[\Phi] + \delta_j[f^{\mathrm{B}}]) \quad \text{for } n \geqslant 4
\end{aligned} \tag{47}$$

Note that, since $\mathscr{D}_n[\Phi] = O(\varepsilon^{n+1})$ and $\delta_n[f^{\mathrm{B}}] = O(\varepsilon^{n+1})$, both Q_n and R_n are $O(\varepsilon^n)$, where ε is the wave slope defined by $\varepsilon = a/\lambda$. In the absence of a body ($f^{\mathrm{B}} \equiv 0$), system (44)–(45) can be reduced, when written in the Fourier space, to that for free waves presented in West *et al.* [9]. For numerical computations, Q and R need to be approximated by truncated series and here the first three approximations will be shown explicitly.

4.1. Linear approximation

For $\varepsilon \ll 1$, by approximating Q and R as $Q \simeq Q_1$ and $R \simeq R_1$, Equations (44)–(45) can be reduced to the first-order equations

$$\frac{\partial \zeta}{\partial t} + \mathscr{L}[\Phi] = f^{\mathrm{B}}, \quad \frac{\partial \Phi}{\partial t} + g\zeta = 0 \tag{48}$$

which can be combined into a single equation for Φ

$$\frac{\partial^2 \Phi}{\partial t^2} - g\mathscr{L}[\Phi] = -f^{\mathrm{B}} \tag{49}$$

4.2. Second-order approximation

By introducing Ψ defined by

$$\Psi(\mathbf{x}, t) = \mathscr{L}[\Phi] - f^{\mathrm{B}}(\mathbf{x}, t) \tag{50}$$

Copyright © 2007 John Wiley & Sons, Ltd.

DOI: 10.1002/fld

and retaining the first two terms of Q and R, the second-order equations can be written as

$$\frac{\partial \zeta}{\partial t} + \Psi + \nabla \cdot (\zeta \nabla \Phi) + \mathscr{L}[\zeta \Psi] = 0 \tag{51}$$

$$\frac{\partial \Phi}{\partial t} + g\zeta + \frac{1}{2}\nabla \Phi \cdot \nabla \Phi - \frac{1}{2}\Psi^2 = 0 \tag{52}$$

4.3. Third-order approximation

Similarly, by neglecting the terms higher than $O(\varepsilon^3)$, the evolution equations correct to third order in wave steepness can be written as

$$\frac{\partial \zeta}{\partial t} + \Psi + \nabla \cdot (\zeta \nabla \Phi) + \mathscr{L}[\zeta \Psi] + \nabla^2 \left(\frac{1}{2}\zeta^2 \Psi \right) + \mathscr{L}\left[\zeta \mathscr{L}[\zeta \Psi] + \frac{1}{2}\zeta^2 \nabla^2 \Phi \right] = 0 \tag{53}$$

$$\frac{\partial \Phi}{\partial t} + g\zeta + \frac{1}{2}\nabla \Phi \cdot \nabla \Phi - \frac{1}{2}\Psi^2 - \Psi(\zeta \nabla^2 \Phi + \mathscr{L}[\zeta \Psi]) = 0 \tag{54}$$

5. NUMERICAL METHOD

Before describing the details of the numerical method, the steps involved at each time step can be summarized as follows: (1) compute the free-surface velocity potential $\phi^{\mathrm{F}}(\mathbf{x}, z, t_n)$ to find the modified body boundary condition given by (30); (2) solve the linear body problem for $\phi^{\mathrm{B}}(\mathbf{x}, z, t_n)$ given by (28)–(30); (3) solve the nonlinear evolution equations (44)–(45) to find $\zeta(\mathbf{x}, t_{n+1})$ and $\Phi(\mathbf{x}, t_{n+1})$.

In the first step, the free-surface variables at $t = t_n$ and the body velocity potential at $t = t_{n-1}$ are assumed to be known from either initial conditions or the solutions from the previous time step. For given $\Phi(\mathbf{x}, t_n)$, $\zeta(\mathbf{x}, t_n)$, and $\phi^{\mathrm{B}}(\mathbf{x}, z, t_{n-1})$, the velocity potential at the mean free-surface $\phi_0(\mathbf{x}, t_n)$ is then computed from (37), which yields, for example, under the third-order approximation

$$\phi_0 = \Phi + \zeta \Psi + \zeta \mathscr{L}[\zeta \Psi] + \tfrac{1}{2}\zeta^2 \nabla^2 \Phi \tag{55}$$

where $\Psi = \mathscr{L}[\Phi(\mathbf{x}, t_n)] - f^{\mathrm{B}}(\mathbf{x}, t_{n-1})$ from (50). Note that the body potential from the previous time step is used to compute f^{B}. This introduces an error of $O(\Delta t)$ with Δt being the time-step size. Alternatively, one could repeat the whole numerical procedure to correct this error but, as shown later, this error is found to be small. Therefore, unless otherwise specified, the results shown in this paper are those without any iteration on f^{B}. After ϕ_0 is computed, ϕ^{F} can be written, in a Fourier series, as

$$\phi^{\mathrm{F}} = \sum_{n=-N_x/2}^{N_x/2} \sum_{m=-N_y/2}^{N_y/2} c_{nm}(t)\, \mathrm{e}^{|\mathbf{K}|z}\, \mathrm{e}^{\mathrm{i}\mathbf{K}\cdot\mathbf{x}} \tag{56}$$

where $c_{nm}(t)$ is the Fourier coefficients of $\phi^{\mathrm{F}}(\mathbf{x}, 0, t_n)$ approximated by $\phi_0(\mathbf{x}, t_n) - \phi^{\mathrm{B}}(\mathbf{x}, 0, t_{n-1})$ and is computed by double FFT. In Equation (56), N_x and N_y are the numbers of Fourier modes in the x- and y-directions, respectively, and $\mathbf{K} = (nk_1, mk_2)$, where $k_1 = 2\pi/L_1$ and $k_2 = 2\pi/L_2$

Copyright © 2007 John Wiley & Sons, Ltd.

DOI: 10.1002/fld

with L_1 and L_2 being the computational domain lengths in the x- and y-directions, respectively. The normal derivative of the free-surface velocity potential on the body surface ($\nabla\phi^{\mathrm{F}} \cdot \mathbf{n}$ on S_{B}) is then computed to find the modified body boundary condition given by (30).

In the second step, with the modified body boundary condition found in the first step, the linear boundary value problem is solved for $\phi^{\mathrm{B}}(\mathbf{x}, z, t_n)$ given by (28)–(30) using the method of a source distribution given by (31). In this paper, to approximate integral (31), we use a desingularized method [12], where point sources are distributed at discrete points $(\mathbf{x}'_j, z'_j)$ displaced slightly into the body in the normal direction from collocation points on the body surface. Here, the offset distance is chosen the average of the two distances between the collocation point and its two neighbours. Then, ϕ^{B} is written as

$$\phi^{\mathrm{B}}(\mathbf{x}, z) = \sum_{j=1}^{N_{\mathrm{B}}} \sigma_j G(\mathbf{x}, \mathbf{x}'_j, z, z'_j) \tag{57}$$

where N_{B} is the number of sources to represent the body. In (57), the Green function G is a periodic array of the source potentials given by (32) or (33) for three- or two-dimensional bodies, respectively. While the explicit form of the two-dimensional source potential in a periodic domain is known [13, Section 13.71] as

$$G = \frac{1}{4\pi} \ln\left[\frac{1}{2}\cosh\left(\frac{2\pi(z-z')}{L}\right) - \frac{1}{2}\cos\left(\frac{2\pi(x-x')}{L}\right)\right] \tag{58}$$

where (x', z') is the location of a source and L is the length of the periodic domain, the periodic three-dimensional source potential has to be computed numerically [14]. Imposing the body boundary condition (30) at the collocation points yields a system of linear algebraic equations for source strength σ_j, which is solved numerically using LU decomposition.

In the final step, the evolution equations (53)–(54) are solved for $\Phi(\mathbf{x}, t_{n+1})$ and $\zeta(\mathbf{x}, t_{n+1})$ after evaluating $\Psi(\mathbf{x}, t_n)$ using the new body potential at $t = t_n$ found in the second step. To solve the system of equations given by (53)–(54), a pseudo-spectral method is used and the free-surface elevation ζ and the free-surface velocity potential Φ are represented in truncated Fourier series

$$\zeta(\mathbf{x}, t) = \sum_n \sum_m a_{nm}(t)\, \mathrm{e}^{\mathrm{i}nk_1x + \mathrm{i}mk_2y}, \quad \Phi(\mathbf{x}, t) = \sum_n \sum_m b_{nm}(t)\, \mathrm{e}^{\mathrm{i}nk_1x + \mathrm{i}mk_2y} \tag{59}$$

Then, all the linear operations are evaluated in the Fourier space, while the product between two functions for the nonlinear terms in the evolution equations will be computed in the physical space. For example, the two linear operators (∇ and $\mathscr{L}[\ ]$) are evaluated in the Fourier space as

$$\nabla(a_{nm}(t)\, \mathrm{e}^{\mathrm{i}\mathbf{K}\cdot\mathbf{x}}) = \mathrm{i}\mathbf{K} a_{nm}(t)\, \mathrm{e}^{\mathrm{i}\mathbf{K}\cdot\mathbf{x}}, \quad \mathscr{L}[a_{nm}(t)\, \mathrm{e}^{\mathrm{i}\mathbf{K}\cdot\mathbf{x}}] = -|\mathbf{K}| a_{nm}(t)\, \mathrm{e}^{\mathrm{i}\mathbf{K}\cdot\mathbf{x}} \tag{60}$$

In order to integrate the evolution equations in time, the fourth-order Runge–Kutta (RK4) scheme or the explicit third-order Adams–Bashforth (AB3) scheme are used with a time step of approximately 5% of the Courant–Fredrichs–Lewey limit. Initial conditions at $t = 0$ for the case of a body in motion are $\Phi(\mathbf{x}, 0) = 0$ and $\zeta(\mathbf{x}, 0) = 0$, since its motion starts from rest, while those for the incident free wave case are exact travelling wave solutions. The details of the numerical method to solve the evolution equations including the numerical beach to absorb waves propagating towards the computational boundaries and a numerical filter to eliminate instability due to aliasing error can be found in Kent [15].

Copyright © 2007 John Wiley & Sons, Ltd.

DOI: 10.1002/fld

The hydrodynamic force on the body is calculated by numerically integrating, using the trapezoidal rule, the dynamic pressure on the body $S_B(t)$ given by

$$p = -\rho\left(\frac{\partial\phi}{s\partial t} + \frac{1}{2}|\nabla_3\phi|^2\right) \tag{61}$$

which can be rewritten as

$$p = -\rho\left[\frac{\partial(\phi|_{S_B})}{\partial t} - \mathbf{V}\bullet\nabla_3\phi + \frac{1}{2}\nabla_3\phi\bullet\nabla_3\phi\right] \tag{62}$$

where $\phi|_{S_B} = \phi^B|_{S_B} + \phi^F|_{S_B}$ is the total velocity potential evaluated at the instantaneous body position. The chain rule for differentiation has been used to rewrite the time derivative of the velocity potential, which is evaluated using a first-order backward difference scheme.

For this method, the operation count per time step is $O(N_F \log N_F + N_B N_F)$ where N_F is the number of points on the free surface and N_B is the number of points on the body, and remains constant regardless of body motion, as demonstrated in Section 6.

While we were unable to compare computation times directly with other numerical methods, the differences between them and our method can be summarized as follows. A MEL-type method would have $O((N_B + N_F)^2)$ operations per time step, mostly due to the evaluation of all the interaction terms between singularities. Though the computational cost of MEL methods can be decreased using numerical approximations, such as multipole acceleration [2], it is inherently a more computationally expensive approach. The MEL method does allow the capture of a breaking wave up to the point of jet re-entry, which is not possible using the present method or a HOS method due to the assumption of a single-valued function of the horizontal coordinate. It should be noted that once the jet does re-enter, MEL computations cannot continue unless an artificial numerical technique to suppress the wave breaking is applied.

The original HOS method of Liu *et al.* [4] has an operation count of $O(N_F \log N_F + N_B N_F)$ per time step after an initial set-up cost of $O(N_B N_F \log N_F + N_B^2 N_F)$. This count appears identical to that for the current approach, but there are several more steps involved in the HOS method: for example, in the HOS method, the boundary value problem (BVP) is set up for points for both the body and the free surface while in the current approach the BVP is only solved on the body where only a small number of collocation points are located. This certainly leads to a much smaller matrix to be evaluated. Also, for the original HOS approach, the whole BVP is solved for each order of nonlinearity, while in our approach, because of the decomposition, we only need to solve for the body potential once per time step. Finally, in the case where the body is moving relative to the free surface and one wishes to capture the motion exactly, the HOS computational cost increases to $O(N_B N_F \log N_F + N_B^2 N_F)$ due to the fact that the set-up step is required at each time step to take into account the change in geometry.

6. NUMERICAL RESULTS

To validate our formulation and numerical method, a two-dimensional flow with a submerged cylinder is considered and our numerical solutions of the one-dimensional version of our system of evolution equations given by (53)–(54) are compared with available analytical and numerical

Copyright © 2007 John Wiley & Sons, Ltd.

DOI: 10.1002/fld

solutions obtained previously. Although we could include an arbitrary order of nonlinearity, we present numerical solutions valid to the third order in wave steepness in this paper.

6.1. Translating submerged circular cylinder

First, we consider a steadily translating circular cylinder in a frame of reference moving with the cylinder, but, as shown in Havelock [16] for an instantaneously created steadily translating pressure, the convergence to a steady state is slow. To avoid this slow convergence, the speed of the moving reference frame is smoothly accelerated up to the final constant speed using

$$U_a(t) = \begin{cases} U\left[1 - \cos^2\left(\dfrac{\pi t}{2T}\right)\right], & t < T \\ U, & t \geqslant T \end{cases} \tag{63}$$

This acceleration scheme decreases the size of the slow oscillation of wave amplitude in time and forces the system to approach the steady-state quickly.

Figures 2–4 show the free-surface elevation due to a circular cylinder of radius $D/R = 5$ moving with speeds $U/(gD)^{1/2} = 0.4, 0.8, 1.2$, where D is the submergence depth of its centre. For the numerical results presented in Figures 2–4, a resolution of $N_F \approx 32$ points/wavelength is used to solve the evolution equations (53)–(54) and the number of sources for the body problem is $N_B = 40$, which are distributed evenly along the circumference. It is found that the numerical solutions for the third-order evolution equations at large times show excellent agreement with the fully nonlinear steady solutions of Scullen and Tuck [17] found numerically using a boundary integral method with a higher resolution, where $N_F \approx 70$/wavelength on the free surface and $N_B = 128$ on the body surface. The second-order solutions compare well with the higher-order solutions for both small

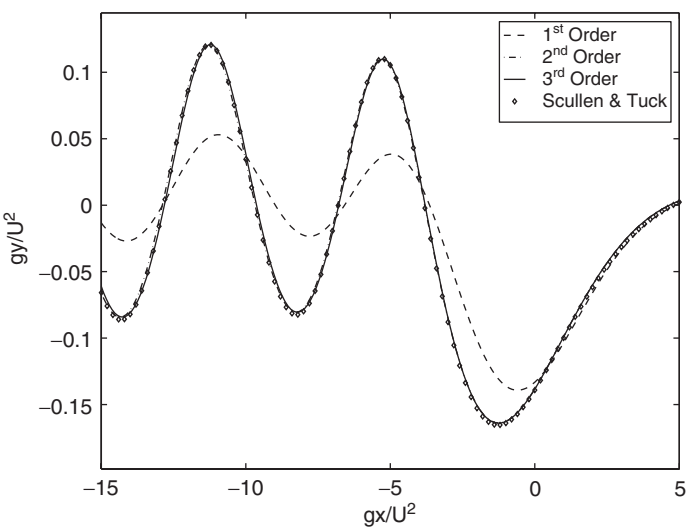

Figure 2. Free-surface elevation of a steadily translating circular cylinder of radius $D/R = 5$ with $U/\sqrt{gD} = 0.4$. The third-order solution (——) is compared with the first- (– –) and second- (- · -) order solutions as well as the fully nonlinear numerical solution of Scullen and Tuck [17] (◇).

Copyright © 2007 John Wiley & Sons, Ltd.

DOI: 10.1002/fld

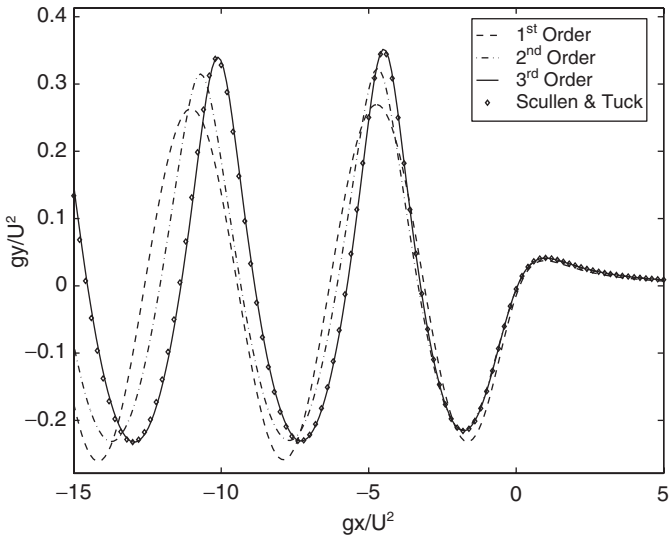

Figure 3. Free-surface elevation of a steadily translating circular cylinder of radius $D/R=5$ with $U/\sqrt{gD}=0.8$. The third-order solution (——) is compared with the first- (– –) and second- (- · -) order solutions as well as the fully nonlinear numerical solution of Scullen and Tuck [17] (◇).

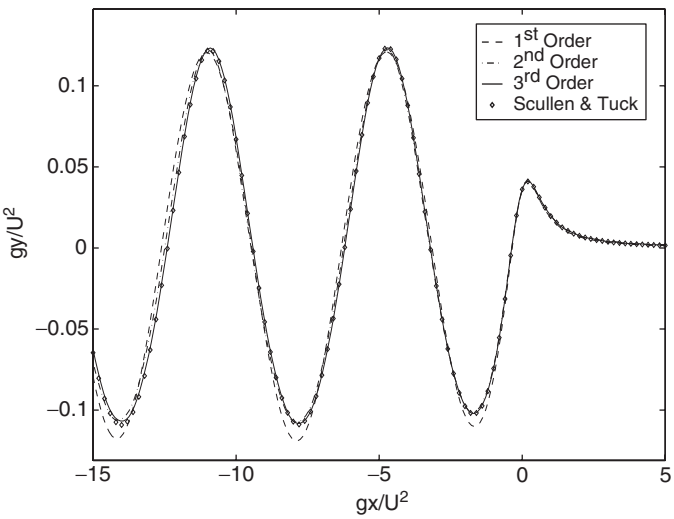

Figure 4. Free-surface elevation of a steadily translating circular cylinder of radius $D/R=5$ with $U/\sqrt{gD}=1.2$. The third-order solution (——) is compared with the first- (– –) and second- (- · -) order solutions as well as the fully nonlinear numerical solution of Scullen and Tuck [17] (◇).

and large depth Froude numbers. For the intermediate depth Froude number of $U/(gD)^{1/2}=0.8$, the wave amplitude is relatively large and the second-order solution becomes a poor approximation. For the case of $U/(gD)^{1/2}=0.4$ and 0.8, one can still observe a large error in the linear solution

Copyright © 2007 John Wiley & Sons, Ltd.

DOI: 10.1002/fld

Table I. Average computational time per time step (T) on a Intel Pentium 4 (3.2 GHz processor) for the translating cylinder case with $D/R=5$, $U/\sqrt{gD}=1.2$, for different resolutions and body motions.

Case description	T (s)	Ratio
$N_F \approx 32$ points/λ, $N_B=40$, fixed	1.21E−002	Base
$N_F \approx 64$ points/λ, $N_B=40$, fixed	2.36E−002	1.95
$N_F \approx 32$ points/λ, $N_B=80$, fixed	2.09E−002	1.72
$N_F \approx 64$ points/λ, $N_B=80$, fixed	3.96E−002	3.27
$N_F \approx 32$ points/λ, $N_B=40$, vertical oscillation ($A/R=0.05$, $\omega^2 R/g=1.0$)	1.23E−002	1.01

when compared with the nonlinear results, verifying the importance of the free-surface nonlinearity in the steady translation problem of a circular cylinder, as pointed out by Tuck [18].

Table I gives a representative sample of computational times for the $U/\sqrt{gD}=1.2$ case for several different combinations of resolutions on the body and free surface. For example, when N_F is increased by a factor of 2 with a fixed N_B, the computational time is almost doubled, which supports our estimated operation count of $O(N_F \log N_F + N_F N_B)$. In the final case in Table I, the result of a vertical oscillation ($A/R=0.05$, $\omega^2 R/g=1.0$) has been introduced to show that the computation cost essentially remains unchanged even if the body is undergoing motion in the reference frame and the solution is on the exact body surface. There was no discernible difference in the free-surface elevations between the various resolutions and hence comparison plots are not presented.

6.2. *Oscillating submerged circular cylinder*

We now examine the problem of a submerged cylinder undergoing heave or circular motion near the mean free surface, which has been extensively studied after the pioneering works by Ursell [19] and Ogilvie [20].

In these numerical computations, the number of points on the body is $N_B=40$ and the resolution on the free surface is $N_F \approx 32$ points/wavelength for both the vertical and the circular motion problems. Our numerical solutions for a fixed submergence depth are first compared with the results of Wu [21] who used the linear free-surface boundary conditions but imposed the exact body boundary condition by expanding the body boundary condition about the mean position of the body.

To determine the harmonic force coefficients, the hydrodynamic force on the cylinder in the jth direction is expressed as a Fourier series in time

$$F_j = Re\left\{\sum_{s=-\infty}^{\infty} f_j(s) e^{is\omega t}\right\} \tag{64}$$

and the force coefficients are obtained as

$$C_j(0) = Re[f_j(0)]/\rho\omega^2\pi R^2 A, \quad C_j(s) = Re[f_j(s) + f_j(-s)]/\rho\omega^2\pi R^2 A \tag{65}$$

Copyright © 2007 John Wiley & Sons, Ltd.

DOI: 10.1002/fld

Table II. Vertical force coefficients for a heaving submerged cylinder with $A/R=0.2$, $\omega^2 R/g=1.0$ and $D/R=3$.

Calculation	$C_3(0)$	$C_3(1)$	$C_3(2)$	$C_3(3)$	$C_3(4)$	$C_3(5)$	$C_3(6)$	$C_3(7)$
Wu [21]	−4.9e−03	8.774e−01	1.e−02	5.e−4	0	0	0	0
First order	−4.872e−03	8.746e−01	9.895e−03	5.080e−04	2.199e−05	1.098e−06	1.728e−07	1.444e−07
Third order	−4.866e−03	8.748e−01	8.500e−03	2.433e−04	3.265e−06	2.697e−07	1.562e−07	1.034e−07

Table III. Vertical force coefficients for a heaving submerged cylinder with $A/R=0.8$, $\omega^2 R/g=1.0$, and $D/R=3$.

Calculation	$C_3(0)$	$C_3(1)$	$C_3(2)$	$C_3(3)$	$C_3(4)$	$C_3(5)$	$C_3(6)$	$C_3(7)$
Wu [21]	−2.05e−02	8.672e−01	4.27e−02	8.8e−03	1.5e−03	3.e−04	0	0
First order	−2.034e−02	8.644e−01	4.212e−02	8.636e−03	1.500e−03	2.443e−04	3.846e−05	5.696e−06
Third order	−2.002e−02	8.679e−01	3.314e−02	3.989e−03	2.093e−04	1.025e−04	4.805e−05	1.569e−05

Table IV. Vertical force coefficients for a heaving submerged cylinder with $A/R=0.2$, $\omega^2 R/g=1.0$ and $D/R=1.3$.

Calculation	$C_3(0)$	$C_3(1)$	$C_3(2)$	$C_3(3)$	$C_3(4)$	$C_3(5)$	$C_3(6)$	$C_3(7)$
First order	2.748e−02	5.520e−01	5.680e−02	5.764e−03	3.077e−03	6.260e−04	1.844e−04	4.838e−05
Third order	6.831e−03	4.924e−01	5.408e−02	4.416e−02	1.166e−02	7.646e−03	8.257e−03	6.169e−03

Table V. Horizontal and vertical force coefficients for a submerged cylinder undergoing clockwise circular oscillations with $A/R=0.6$, $\omega^2 R/g=0.5$, and $D/R=3$.

Calculation	$C_1(0)$	$C_1(1)$	$C_1(2)$	$C_1(3)$	$C_1(4)$	$C_1(5)$	$C_1(6)$	$C_1(7)$
Wu [21]	−4.19e−02	8.843e−01	3.92e−02	6.2e−03	9.e−04	1.e−04	0	0
First order	−4.128e−02	8.812e−01	3.896e−02	6.191e−03	9.236e−04	1.241e−04	1.511e−05	1.711e−06
Third order	−3.937e−02	8.825e−01	3.753e−02	4.072e−03	4.370e−04	3.468e−05	4.007e−06	1.052e−06
Calculation	$C_3(0)$	$C_3(1)$	$C_3(2)$	$C_3(3)$	$C_3(4)$	$C_3(5)$	$C_3(6)$	$C_3(7)$
Wu [21]	−7.0e−03	8.859e−01	3.86e−02	6.2e−03	9.e−04	1.e−04	0	0
First order	−6.895e−03	8.828e−01	3.840e−02	6.132e−03	9.182e−04	1.237e−04	1.511e−05	1.648e−06
Third order	−8.247e−03	8.824e−01	3.745e−02	4.078e−03	4.434e−04	3.574e−05	3.308e−06	5.677e−07

where ω is the frequency of oscillation, R is the radius of the circular cylinder, and A is the amplitude of the motion. In the results presented here, the cylinder, with centre submergence D, is allowed to oscillate through two full periods to remove any initial transients and the problem is assumed to have reached a limit cycle. The force history is then recorded for 32 periods and this time history is analysed using a Fourier transform for the results in Tables II–V.

Copyright © 2007 John Wiley & Sons, Ltd.

DOI: 10.1002/fld

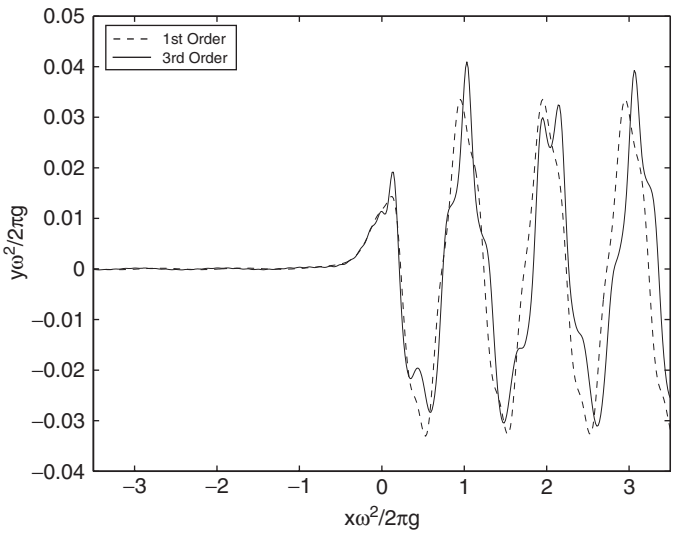

Figure 5. First- (– –) and third-order (——) free-surface elevations due to a submerged circular cylinder undergoing clockwise circular oscillations with $D/R = 3$, $\omega^2 R/g = 0.5$, $A/R = 0.6$, and $t\omega/2\pi = 39$.

Tables II and III compare the linear and nonlinear results for the force coefficients on a submerged cylinder undergoing small and large amplitude vertical oscillations. The first-order solutions show good agreement with Wu's solutions except in the higher harmonic components which are still nonzero even in the first-order solutions since the exact body boundary condition is imposed. The small difference between the two linear solutions in the higher harmonic force coefficients can be understood from the fact that the full body boundary condition is imposed numerically in the present method, while Wu's results are based on a truncated series. As the amplitude of motion increases, the linear results for the second or higher harmonics are expected to be no longer accurate and the third-order solutions show the importance of the free-surface nonlinearity, which has been neglected in Wu's computations. In general, one can note that the linear solutions overestimate the vertical force coefficients.

Table IV presents results for a heaving cylinder moving as close as 10% of a radius to the mean free surface. Unlike the results in Table II, even for small amplitude motion, the mean and higher harmonic force coefficients are significantly different from the linear results, indicating that nonlinearity becomes important as the submergence depth decreases.

Table V presents the results for the same circular cylinder undergoing a clockwise circular motion. Once again, the numerical and analytical linear results show good agreement and the nonlinear free-surface effects appear at the second harmonic or higher, as expected. Figure 5 shows the first- and third-order free-surface elevations at the end of the computation. As predicted by the linear theory of Ogilvie [20], the waves travelling to the right are much larger than those travelling to the left, which is also consistent with the nonlinear predictions of Liu *et al.* [6]. Note that, while both the linear and nonlinear computations result in nonsinusoidal wave forms, driven mostly by large amplitude motions of the cylinder close to the free surface, the development of higher harmonics is more apparent in the third-order solution.

Copyright © 2007 John Wiley & Sons, Ltd.

DOI: 10.1002/fld

6.3. Fixed cylinder beneath incoming waves

The problem of a fixed horizontal cylinder under the free surface with incident waves has been studied, for example, experimentally by Chaplin [22] and Grue [23], analytically by Ogilvie [20], Palm [24] and Liu *et al.* [6] in the frequency domain, and numerically by Liu *et al.* [4] in the time domain. Here, the force coefficients on a circular cylinder of radius R with centre submergence depth $D/R=2$ from the undisturbed free surface are computed and compared with the results of Liu *et al.* [4] who used a HOS method.

As the initial condition, an exact Stokes wave solution calculated using the method described by Choi and Camassa [25] is used and, at $t=0+$, the body boundary condition is suddenly enforced. To eliminate any transient response, computations are carried out for 10 wave periods and the results shown below are obtained from the last three wave periods of computation. The computational domain on the free surface is 16 incident wavelengths long, with a resolution of 128 points per wavelength and the number of singularities on the body is $N_B=40$. A higher number of body points was also attempted, e.g. $N_B=256$ for one case, but no significant improvement in the result was observed. The fourth-order Runge–Kutta scheme is used for time integration with 128 time steps per wave period of the incident wave.

The numerical results for two different incoming wave slopes are compared with the previous results. As shown in Table VI, for $kR=0.4$ and $ka=0.08$, where k is the wave number and a is the wave amplitude, the first- and third-order results for the first and second harmonic force coefficients are in good agreement with the linear result of Ogilvie [20], and the nonlinear results of Liu *et al.* [4], respectively. Although the comparison for the mean horizontal force over one period, $f_1(0)$, seems to be reasonable in this comparison, the computation shows the mean value is sensitive to the sampling period and varies with the initial time for sampling. This is contrary to what Liu *et al.* [4] reported, but the source of this discrepancy is not clearly understood yet. To ensure that the error introduced when using the body velocity potential (ϕ^B) at the previous time step to compute ϕ_0 (see Equation (55)) is small and is not the cause of the variation in the mean drift force, a new calculation for the case shown in Table VI is carried with one or two iterations on ϕ^B whenever the modified body boundary condition is computed. The errors on the harmonic force coefficients are found to be less than 1%, while the same fluctuation in the drift force with the error of less than 5% is observed.

Another case computed is for a longer and larger wave of $kR=0.206$ and $ka\simeq 0.099$, or equivalently $K_c=1.0$, where the Keulegan–Carpenter number K_c is defined by

$$K_c=\frac{\pi a}{R}\mathrm{e}^{-kD} \tag{66}$$

Table VI. Horizontal force coefficients for a submerged circular cylinder in incident Stokes waves with $D/R=2$, $kR=0.4$, and $ka=0.08$.

	Ogilvie [20]	Liu *et al.* [4]	Present (first order)	Present (third order)
$f_1(1)/(\rho g R a)$	1.15	1.1406 (first order)	1.1554	1.1342
$f_1(2)/(\rho g a^2)$	—	0.2754 (second order)	—	0.2919
$f_1(0)/(\rho g k^2 a^4)$	—	−1.0561 (fourth order)	—	−0.9910

Copyright © 2007 John Wiley & Sons, Ltd.

DOI: 10.1002/fld

Table VII. Horizontal force coefficients for a submerged circular cylinder in incident Stokes waves with $D/R = 2$, $kR = 0.206$, and $Ka = 0.099$ (or $K_c = 1.0$).

	Chaplin [22] Experiment	Liu *et al.* [4] Fourth order	Present method Third order
$f_1(1)/(\rho\omega^2 R^3 K_c)$	1.5	2.275	2.2167
$\ln(f_1(2)/(\rho\omega^2 R^3))$	−1.5	−1.0	−1.0788
$\ln(f_1(3)/(\rho\omega^2 R^3))$	−2.6	−2.5	−2.4181

for which both the experimental results of Chaplin [22] and the numerical results of Liu *et al.* [4] are available. As shown in Table VII, the present results agree well with the previous numerical results of Liu *et al.* [4], but exhibits the same error on the first harmonic force coefficient when compared to Chaplin [22], which can be attributed to viscous effects [4, 22].

7. DISCUSSION

An explicit nonlinear formulation to solve unsteady wave–body interaction problems in an ideal fluid of infinite depth has been presented. After decomposing the total velocity potential into the body and free-surface velocity potentials, it has been shown that the body velocity potential can be found by solving the simplified boundary value problem in an unbounded fluid domain, while the free-surface problem is reduced to a system of two coupled nonlinear evolution equations. This system is then solved using an efficient pseudo-spectral method to update the free-surface elevation and the total velocity potential at the free surface, while the simplified body problem is solved using a desingularized boundary integral method. Numerical solutions for a submerged circular cylinder have been presented to demonstrate the capability of our method to solve the translation, radiation, and diffraction problems. The results were validated against other theoretical or numerical results, showing good agreement.

Advantages of the formulation presented here compared with other approaches can be summarized as follows. First, it is necessary to solve the linear body problem in an unbounded domain only once per time step, regardless of the order of free-surface nonlinearity to be included in the free surface. Secondly, after the body velocity potential is found, the system of two evolution equations is explicitly written in terms of two free-surface variables and, therefore, there are no extra numerical steps to close the system before updating the free-surface information.

In this paper, only results for the two-dimensional wave–body interaction problem in infinitely deep water have been presented, but the formulation and the numerical method can be readily applied to solve more general problems. For example, the finite water depth effects can be easily incorporated in our formulation, as described in the Appendix. For a three-dimensional body, the numerical evaluation of the doubly periodic source potential is required and this could be efficiently carried out, for example, using the Ewald summation [14, 26] developed to compute the Coulomb potential for a lattice of point charges. Although it is not discussed in this work and further improvements are desirable, it is shown in Kent [15] that the method can be readily extended to surface piercing bodies. These improvements are underway and will be presented in the future.

Copyright © 2007 John Wiley & Sons, Ltd.

DOI: 10.1002/fld

APPENDIX A: FINITE WATER DEPTH

Though not explicitly considered in this paper, the generalization of our formulation to constant finite water depth is straightforward. The evolution equations remain unchanged when the linear operator $\mathscr{L}$ (defined in Equation (26) for the infinite depth case) is redefined, when acting on a Fourier component, as

$$\mathscr{L}[\mathrm{e}^{\mathrm{i}\mathbf{k}\cdot\mathbf{x}}] = -k\tanh(kh)\,\mathrm{e}^{\mathrm{i}\mathbf{k}\cdot\mathbf{x}} \tag{A1}$$

where h is the water depth. When solving the boundary value problem for the body velocity potential ϕ^{B}, the boundary condition in Equation (29) is replaced by

$$\frac{\partial\phi^{\mathrm{B}}}{\partial z} = 0 \quad \text{at } z = -h \tag{A2}$$

which can be easily satisfied through the use of image potentials. For example, instead of (58), the Green function G satisfying (A2) can be written as

$$\begin{aligned} G = {} & \frac{1}{4\pi}\ln\left[\frac{1}{2}\cosh\left(\frac{2\pi(z-z')}{L}\right) - \frac{1}{2}\cos\left(\frac{2\pi(x-x')}{L}\right)\right] \\ & + \frac{1}{4\pi}\ln\left[\frac{1}{2}\cosh\left(\frac{2\pi(z-(-2h-z'))}{L}\right) - \frac{1}{2}\cos\left(\frac{2\pi(x-x')}{L}\right)\right] \end{aligned} \tag{A3}$$

Similarly, the summation defined in Equation (56) is changed to

$$\phi^{\mathrm{F}} = \sum_n \sum_m c_{nm}(t)\frac{\cosh(|\mathbf{K}|(z+h))}{\cosh(|\mathbf{K}|h)}\,\mathrm{e}^{\mathrm{i}\mathbf{K}\cdot\mathbf{x}} \tag{A4}$$

ACKNOWLEDGEMENTS

The authors gratefully acknowledge support from the US Office of Naval Research through Grant N00014-05-1-0537.

REFERENCES

1. Longuet-Higgins M, Cokelet E. The deformation of steep surface waves in water. I. A numerical method of computation. *Proceedings of the Royal Society of London A* 1976; **350**:1–26.
2. Beck R, Reed AM. Modern computational methods for ships in a seaway. *SNAME Transactions* 2001; **109**:1–52.
3. Liu Y, Xue M, Yue DKP. Computations of fully nonlinear three-dimensional wave–wave and wave–body interactions. *Journal of Fluid Mechanics* 2001; **438**:41–66.
4. Liu Y, Dommermuth DG, Yue DKP. A high-order spectral method for nonlinear wave–body interactions. *Journal of Fluid Mechanics* 1992; **245**:115–136.
5. Dommermuth D, Yue D. A high-order spectral method for the study of nonlinear gravity waves. *Journal of Fluid Mechanics* 1987; **184**:267–288.
6. Liu Y, Zhu Q, Yue DKP. Nonlinear radiated and diffracted waves due to the motions of a submerged circular cylinder. *Journal of Fluid Mechanics* 1999; **382**:263–282.
7. Lin RQ, Kuang W. Nonlinear waves of a steadily moving ship in environmental waves. *Journal of Marine Science and Technology* 2004; **8**:109–116.

Copyright © 2007 John Wiley & Sons, Ltd.

DOI: 10.1002/fld

8. Choi W. Nonlinear evolution equations for two-dimensional waves in a fluid of finite depth. *Journal of Fluid Mechanics* 1995; **295**:381–394.
9. West BJ, Brueckner KA, Janda RS, Milder DM, Milton RL. A new numerical method for surface hydrodynamics. *Journal of Geophysical Research* 1987; **92**:11803–11824.
10. Choi W, Kent CP. A pseudo-spectral method for nonlinear wave hydrodynamics. *Proceedings of 25th ONR Symposium*, St. John's Newfoundland, 2004.
11. Choi W, Kent CP, Schillinger CJ. Numerical modeling of nonlinear surface waves and its validation. *Advances in Engineering Mechanics—Reflections and Outlooks in honor of Theodore Y.-T. Wu*. World Scientific: Singapore, 2005; 94–110.
12. Cao Y, Beck R, Schultz W. An three-dimensional desingularized boundary integral methods for potential problems. *International Journal for Numerical Methods in Fluids* 1993; **12**:785–803.
13. Milne-Thompson LM. *Theoretical Hydrodynamics*. Dover: New York, 1938.
14. Baker GR, Meiron DI, Orszag SA. Boundary integral methods for axisymmetrical and three-dimensional Rayleigh–Taylor instability problems. *Physica* 1984; **12D**:19–31.
15. Kent CP. A pseudo spectral method for calculating wave–body interaction using an explicit free-surface formulation. *Thesis*, Department of Naval Architecture and Marine Engineering, University of Michigan, 2005.
16. Havelock T. The initial wave resistance of a moving surface pressure. *Proceedings of the Royal Society of London A* 1917; **93**:240–253.
17. Scullen D, Tuck EO. Nonlinear free-surface flow computations for submerged cylinders. *Journal of Ship Research* 1995; **39**:185–193.
18. Tuck EO. The effect of non-linearity at the free surface on flow past a submerged cylinder. *Journal of Fluid Mechanics* 1965; **22**:401–414.
19. Ursell F. Surface waves on deep water in the presence of a submerged circular cylinder. *Proceedings of the Cambridge Philosophical Society* 1950; **46**:141–152.
20. Ogilvie TF. First, second order forces on a cylinder under a free surface. *Journal of Fluid Mechanics* 1963; **16**:451–472.
21. Wu GX. Hydrodynamic forces on a submerged circular cylinder undergoing large-amplitude motion. *Journal of Fluid Mechanics* 1993; **254**:41–58.
22. Chaplin JR. Nonlinear forces on a horizontal cylinder beneath waves. *Journal of Fluid Mechanics* 1984; **147**: 449–464.
23. Grue J. Nonlinear water waves at a submerged obstacle or bottom topography. *Journal of Fluid Mechanics* 1992; **244**:455–467.
24. Palm E. Nonlinear wave reflection from a submerged circular cylinder. *Journal of Fluid Mechanics* 1991; **233**:49–63.
25. Choi W, Camassa R. Exact evolution equations for surface waves. *Journal of Engineering Mechanics* 1999; **125**:756–760.
26. Toukmaji T, Board J. Ewald summation techniques in perspective: a survey. *Computational Physics Communications* 1996; **95**:73–92.

Copyright © 2007 John Wiley & Sons, Ltd.

DOI: 10.1002/fld